

# We are IntechOpen, the world's leading publisher of Open Access books Built by scientists, for scientists

5,600

Open access books available

137,000

International authors and editors

170M

Downloads

Our authors are among the

154

Countries delivered to

TOP 1%

most cited scientists

12.2%

Contributors from top 500 universities



WEB OF SCIENCE™

Selection of our books indexed in the Book Citation Index  
in Web of Science™ Core Collection (BKCI)

Interested in publishing with us?  
Contact [book.department@intechopen.com](mailto:book.department@intechopen.com)

Numbers displayed above are based on latest data collected.  
For more information visit [www.intechopen.com](http://www.intechopen.com)



## Chapter

# A High Fidelity Transmural Anisotropic Ventricular Tissue Model Function to Investigate the Interaction Mechanisms of Drug: An In-Silico Model for Pharmacotherapy

*Srinivasan Jayaraman and Ponnuraj Kirthi Priya*

## Abstract

A high fidelity transmural anisotropic ventricular tissue model consisting of endocardial, mid myocardial, and epicardial myocytes were configured to investigate drug interaction, such as Hydroxychloroquine (HCQ), under hypoxia conditions without and with pro-arrhythmic comorbidity like hypokalemia in (a) ventricular tissue b) its arrhythmogenesis for different dosages and (b) two different pacing sequences (Normal and tachycardiac). In-silico ventricular modeling indicates HCQ has an insignificant effect on hypoxia with and without comorbidities, except in the combination of mild hypoxia with moderate hypokalemia condition and severe hypoxia with mild hypokalemia where it initiated a re-entrant arrhythmia. Secondly, incorporating drug dosage variations indicates the 10  $\mu\text{M}$  HCQ created PVCs for all settings except in severe hypoxia conditions where re-entrant arrhythmia occurred. In addition to the dosage of HCQ utilized for treatment, the pacing protocol also influences the appearance of re-entrant arrhythmia only for severe hypoxia with 10  $\mu\text{M}$  HCQ dosage alone. For all other conditions, including tachycardiac pacing protocol, no arrhythmia occurred. These findings infer that the arrhythmic fatality rate due to HCQ treatment for hypoxia can be effectively alleviated by subtly altering or personalizing the dosage of HCQ and aid in the treatment of hypoxia-induced symptoms caused by COVID.

**Keywords:** Hydroxychloroquine, Hypoxia, Hypokalemia, Azithromycin, Ventricular Arrhythmia, Transmural Tissue, COVID-19

## 1. Introduction

Precision medicine is significantly focused and promoted due to the development of next-generation sequencing, which implies high throughput and lower cost. Even though molecular and cell biology has improved basic understanding of many diseases, novel and pandemic diseases like Severe Acute Respiratory Syndrome Coronavirus (SARS-CoV-2) have many unanswered questions on infection

mechanism, progression, and impact of symptom-based treatment using “off label” drugs. For instance, Hydroxychloroquine (HCQ), an antimalarial drug widely used to boost the immune system, was attempted or explored towards treating COVID-19. The US Food and Drugs Administration (FDA) and WHO initially approved HCQ as an emergency medicine based on laboratory and clinical studies data. Irrespective of earlier findings suggesting that long-term (over 5 years) intake of HCQ is likely to contribute to the development of retinopathy, include QRS widening, QT interval prolongation, ventricular arrhythmias like Torsades de pointes (TdP), hypokalemia and hypotension [1, 2], in-vitro studies reported the potential activity of HCQ on SARS-CoV-2 [3, 4]. On a positive note, in experiments performed on mouse atria, Capel et al. [5] reported that HCQ acted as a bradycardiac agent (reducing the spontaneous beating rate) in sinoatrial cells via a dose-dependent reduction of multiple ionic currents: ‘funny’ current ( $I_f$ ), L-type calcium current ( $I_{CaL}$ ) and rapid delayed rectifier potassium current ( $I_{Kr}$ ). Modeling of drug cardiotoxicity at the cellular level focuses predominantly on reducing  $I_{Kr}$  current and leads to prolongation of APD in cells and QT interval in whole heart level, thereby leading to arrhythmias like TdP [6]. However, a clinical study in France [7] reported that either HCQ alone or in combination with azithromycin is efficient in treating COVID-19. However, Sarkar et al., 2012 [8] reported that one population of cell differs from another (i.e. healthy vs. diseased) and electrophysiological variability manifests at each level, from molecular, cellular, organ, and organism level. Hence, considering the outcome of previous clinical evidence of HCQ on normal cells may be inadequate to provide the exact impact of the effect of HCQ on virus infected cells or tissue. As our particular interest is in the human cardiac system; specifically electrophysiology, we wish to emphasize the variability of COVID-19 in cardiac system. Clinical observations reported by Mercuro et al. [9] shows the median baseline  $QT_c$  was 455 ms in 90 COVID-19 patients and in presence of HCQ, it increased to 473 ms. Among those who received HCQ alone, 19% had  $QT_c$  prolongation of 500 ms or more, 13% had a change in  $QT_c$  of 60 ms or more and 1 case of Torsade de Pointes (TdP) was reported. Thus it’s very evident that investigating and understanding the cardiac manifestation mechanism due to medication like HCQ drug is critical.

Li X et al.’s study in 2019 on 175 patients with COVID-19 reported that, 39 patients had severe hypokalemia (under 3 mmol/L), 69 had moderate hypokalemia (3–3.5 mmol/L) and 67 were normokalemia (over 3.5 mmol/L) [10]. He et al., [11] proposed that ACE-2 signaling pathways may play a role in cardiac injury while hypoxemia caused by COVID-19 may cause damage to myocardial cells. Severe hypoxemia occurring in lungs of COVID-19 patients has been linked to loss of lung perfusion regulation and hypoxic vasoconstriction [12]. Acute viral infections like that of COVID-19 have been known to cause type 1 or 2 myocardial infarction though the frequency of STE in these patients is unclear [13]. All these resulted in the liberal use of HCQ globally, in spite of contempt of paucity of evidence and adverse effect [3] for a short span of time.

During this situation, Wang et al. reported that treating COVID-19 with a combination of HCQ and AZM elicited electrical alternates, re-entrant circuits and the wave breaks [14]. Further, this clinical study reported that different dosages of HCQ blocked the various ionic currents:  $I_{Na}$ ,  $I_{CaL}$ ,  $I_{Kr}$  and  $I_{K1}$  with different intensity. Based on the [15] finding, HCQ treatment for COVID-19 lead to ventricular arrhythmia and death in hospitalized COVID patients, In May 2020, WHO suspended the emergency usage of HCQ; later, this study article was retracted due to reporting of fabricated data. There is no clinical evidence that provides the detailed mechanism of HCQ’s safety or adversity, particularly the cardiac cell and tissue, i.e., under what scenarios the target drug interaction may cause arrhythmias in patients.

Although various researchers have attempted to study the pharmacokinetics of HCQ: it's the inhibitory mechanism on human cells under normal conditions and various abnormal pathologies, for the reasons noted, it is critical to zero down the effect of a drug and explains its response range. Such comprehensive study, either using in-vivo or clinical studies, is difficult in a short period with present-day technology. In this situation, computational models can help to elucidate and overcome the following aspects:

- The effect of COVID-19 infection on electrophysiological properties of ventricular tissue
- Lack of clinical evidence that provides a detailed influence of HCQ on COVID-19 infected cardiac tissue. For example, changes in ECG, mechanism, and potential severity of ventricular arrhythmias like TdP
- Mechanistic understanding of HCQ on ventricular tissues under comorbid scenarios, such as varying intensities of hypokalemia.

To address the above gaps, we develop a 2D transmural anisotropic ventricular tissue model framework that can help in primarily understanding the COVID-19 effect on the ventricular tissue, including the response to pharmacological agents like HCQ. Two variations of COVID-19; mild and severe infection are explored. Secondly, different levels of hypokalemia (mild, moderate and severe) along with COVID-19 are introduced one at a time to understand its effect on ventricular tissue. In each case, the variations in the QT interval and T-peak are recorded. Finally, the tissue is excited with premature stimuli to analyze under which of the above three conditions the tissue becomes pro- arrhythmic. Although studies have established that HCQ induces QT prolongation, TdP arises only in certain scenarios. This study is an attempt to address the possibilities under which an arrhythmia is generated at the tissue level in presence of the above mentioned conditions.

## 2. Transmural cardiac tissue model

The 2D transmural section of the ventricular wall, is represented by an array of  $250 \times 100$  cells, consisting of endocardial (endo), midmyocardial (M) and

Condition	Ionic current	Change
HCQ	$I_{Kr}$	35% reduction
	$I_{CaL}$	12% reduction
Hypokalemia1	$K_o^+$	85% reduction
Hypokalemia2	$K_o^+$	55% reduction
Hypokalemia3	$K_o^+$	45% reduction
Mild COVID-19	$[ATP]_i$	5.5 mM
	$k_{0.5}$	0.125
Severe COVID-19	$[ATP]_i$	5 mM
	$k_{0.5}$	0.250

**Table 1.**  
 Change in parameters for different conditions.

epicardial(epi) cells. The depolarisation and repolarisation patterns generated from the tissue are validated by simulating pseudo ECGs. The action potentials of different types of cardiomyocytes are described by the Ten Tusscher (TP06) model [16]. A stimulus current of amplitude  $52 \mu A$  is applied for 1 ms is used to excite specific cell. The parameters of the model, tissue characteristics and integration scheme are adopted from Priya et al., 2017 [17]. The change in cardiomyocyte's ionic current parameters in the various configurations: hypokalemia and COVID-19 are summarized in **Table 1**.

As COVID-19 has been linked to causing hypoxemia [11], which in turn leads to hypoxia, this condition was included in the cardiac myocytes by increasing intracellular ATP concentration which would in turn lead to activation of an ATP sensitive potassium current. Using the formulation of Shaw and Rudy [18], ATP activated  $K^+$  current is described by the following formula

$$I_{ATP} = G_{k,ATP} \frac{1}{1 + \left(\frac{[ATP]_i}{k_{0.5}}\right)^H} \left(\frac{[K^+]_o}{5.4}\right)^n (V_m - E_k) \quad (1)$$

where  $G_{k,ATP}$  is the maximum conductance of  $I_{ATP}$  current and has a value of  $3.9 \text{ nS/cm}^2$ , H and n have a value of 2 and 0.24 respectively. The intracellular ATP concentration ( $[ATP]_i$ ) under normal condition is 6.8 mM, but it decreases to 5.5 mM in mild hypoxia and 5 mM in severe hypoxia respectively. Similarly,  $k_{0.5}$  is 0.042 for normal condition, 0.125 and 0.25 for mild and severe hypoxia respectively [19]. Henceforth, in this study, hypoxia would be referred as COVID-19 condition. Further, reduction in the rapid delayed rectifying potassium current ( $I_{Kr}$ ) and  $I_{CaL}$  by 35% and 12% respectively in atrial cells as reported by [5] is adapted in our model.

To investigate the benefits and adverse effects of HCQ under control, COVID-19 and comorbid hypokalaemia, the ion channel variations corresponding to these conditions were included in the cells of the tissue one at a time, as reported by [10], the extracellular potassium concentration ( $K_o^+$ ) is reduced by three stages: 85% as hypokalemia1 (mild), 55% as hypokalemia2 (moderate) and 45% as hypokalemia3 (severe). A regular pacing pulse of 800 ms (corresponding to 75 beats per minute) is applied in the tissue, and the corresponding voltage propagation is analyzed. Further, pseudo ECGs are generated for each of the clinical conditions. The variation in ECG, in particular the QT interval and T-wave morphology, both without and with HCQ and in presence of comorbidity is considered for analysis. Furthermore, the tissue is stimulated with premature stimuli in between the normal beats to study which conditions can initiate or sustain an arrhythmia.

### 3. Cardiac tissue mechanism(s) in control, COVID-19 and hypokalemia conditions, and with HCQ

To understand the spatiotemporal mechanism of the cardiac tissue, the lower leftmost corner (Cells 1:10,1:2) of the transmural tissue is stimulated. As a result of this stimuli, a convex wavefront propagates from the endo to mid and epi layer from the bottom to the top of the tissue. The repolarisation occurs first in the epi and endo layers, and M-cells in the mid layer are the last to repolarise. Normalized pseudo ECGs are synthesized from this tissue. *Mild* and *severe* COVID-19 conditions are introduced in the tissue to study its effect without and with HCQ. Furthermore, a comorbidity like hypokalemia is included to understand its influence on COVID-



19 conditions. Pseudo ECGs are synthesized for each of these conditions and the QT interval and T-peak are tabulated in **Table 2**.

In control conditions, a 0.345 sec QT interval and 0.2265 mV T-peak occurs. While in *mild* COVID-19, the QT interval and T-peak decreases by 5.79% (0.325) sec and 33.33% (0.151 mV) respectively as seen in **Figure 1(i)**. In combination with HCQ, the QT interval slightly increases by 1.45% (0.340 sec) and T-peak rises by 20.08% (0.181 mV) in comparison with no HCQ. However, it does not reach the control values. Under severe COVID-19 conditions, the QT interval is further reduced by 20.29% (0.275 s) and a negative T-wave peak of  $-0.17$  mV is observed along with a QT depression. This negative T-peak might be representative of ischemia in clinical ECG recordings. In contrast, the effect of HCQ in *severe* COVID-19 is negligible with unchanged QT interval and slight increase in T-peak ( $-0.153$  mV). Here, we have considered a pacing interval of 800 msec (i.e HR is 75 beats/min), so the Bazett  $QT_c$  interval is 0.363 sec and 0.307 sec in *mild* and *severe* COVID-19 conditions. Anttonen *et al.*, [20] reported that an individual's  $QT_c$  interval  $< 320$  msec is a low rate of all-cause mortality, from which we infer that a patient with *severe* hypoxia is thus not at high risk of mortality from cardiac failure or disorder; unless and otherwise in presence of other comorbidities. On adding HCQ, 0.380 sec

Condition	QT interval (s)	T-peak (mV)
Control	0.345	0.2265
Mild COVID-19	0.325	0.152
Severe COVID-19	0.275	-0.170
Mild COVID-19 with HCQ	0.340	0.181
Severe COVID-19 with HCQ	0.275	-0.153
Hypokalemia1	0.355	0.229
Hypokalemia1 with HCQ	0.375	0.265
Hypokalemia2	0.380	0.217
Hypokalemia2 with HCQ	0.410	0.255
Hypokalemia3	0.390	0.210
Hypokalemia3 with HCQ	0.425	0.246
Hypokalemia1a and Mild COVID-19	0.335	0.127, 0.153
Hypokalemia1 and Mild COVID-19 with HCQ	0.350	0.186
Hypokalemia1 and Severe COVID-19	0.285	-0.16, -0.087
Hypokalemia1 and Severe COVID-19 with HCQ	0.285	-0.14
Hypokalemia2 and Mild COVID-19	0.355	0.141
Hypokalemia2 and Mild COVID-19 with HCQ	0.38	0.174
Hypokalemia2 and Severe COVID-19	0.300	-0.156
Hypokalemia2 and Severe COVID-19 with HCQ	0.305	-0.126
Hypokalemia3 and Mild COVID-19	0.365	0.133
Hypokalemia3 and Mild COVID-19 with HCQ	0.395	0.168
Hypokalemia3 and Severe COVID-19	0.31	-0.155
Hypokalemia3 and Severe COVID-19 with HCQ	0.32	-0.121

**Table 2.**

*Pseudo ECG parameters: T-peak and QT interval duration as a metric for assessing the effect of COVID-19, other comorbidity and in presence of HCQ.*

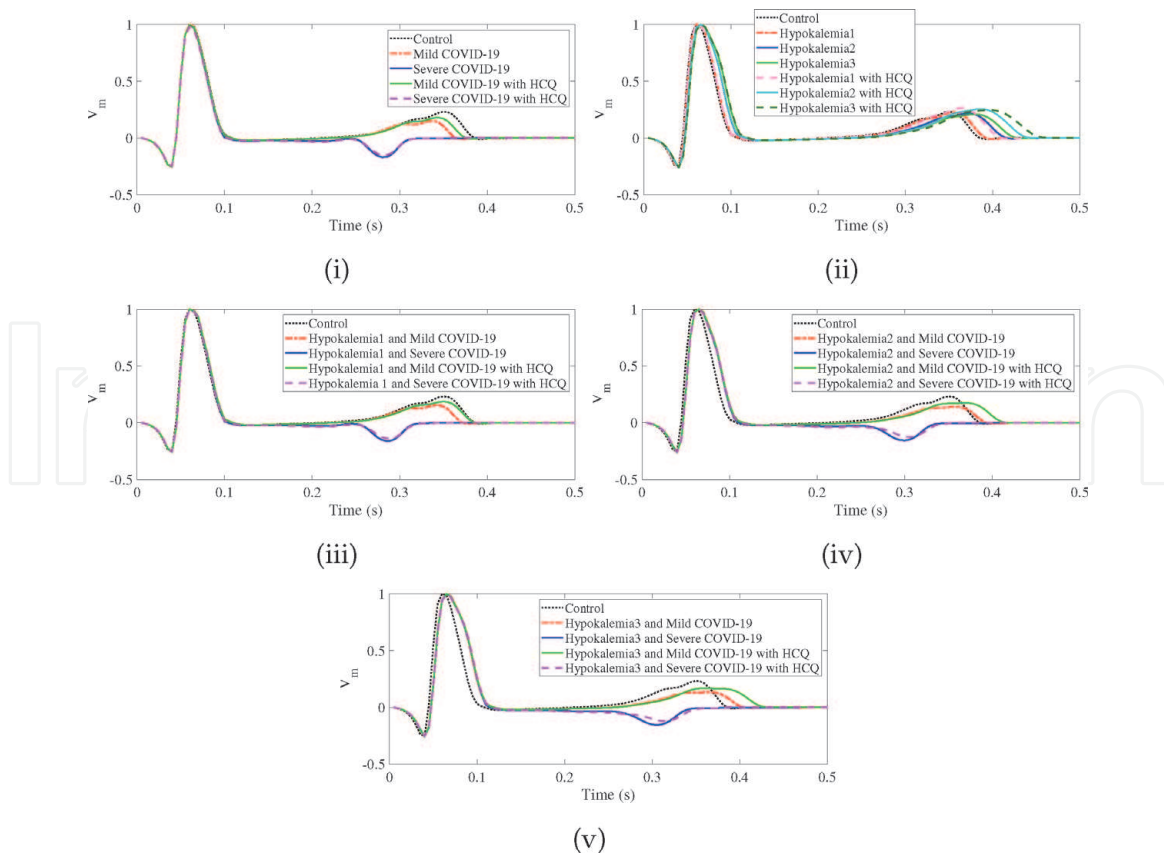


**Figure 1.**

Pseudo ECGs generated in control and in presence of HCQ under (i) mild and severe COVID-19 (ii) Hypokalemia, (iii) Hypokalemia1 and COVID-19, (iv) Hypokalemia2 and COVID-19 and (v) Hypokalemia3 and COVID-19.

$QT_c$  interval increased in *mild*, while it remains the same in *severe* hypoxia conditions. Mercurio et al. [9] reported that in 90 COVID-19 patients, the median baseline  $QT_c$  was 455 (430–474) ms in control vs. 473 [454–487] ms in HCQ conditions. The  $QT_c$  values reported in our study are lower than those observed clinically due to the limitation of considering only a segment of the ventricle. However, the percentage increase in APD between control and HCQ in the clinical study of Mercurio et al. is 3.95%. An increase of 4.68%  $QT_c$  is observed, on comparing the *mild* COVID-19 and on HCQ inclusion.

**Figure 1(ii-v)** shows the pseudo ECGs generated for the different combinations of Hypokalemia and COVID-19 as well as in presence of HCQ. In comorbid hypokalemia1 condition as seen in **Figure 1(ii)**, the QT interval increases by 2.89% (0.355 s), while the peak amplitude of T-wave increases only by 1.10% (0.229 mV), almost similar to control condition. When exposed to HCQ, the QT interval increases by 8.69% (0.375 ms) and T-peak amplitude increases by 16.99% (0.265 mV) in comparison to control. But, when infected by mild COVID-19, the QT interval decreases by 2.89% (0.335 s), yet a notched T-wave appears with the first T-peak of 0.127 mV and second peak of 0.153 mV is observed. On adding HCQ, the notched T-wave are replaced by positive T-waves. The QT interval is increased by 1.45% (0.350 mV) and T-peak is reduced by 17.88% (0.186 mV) in comparison with control. In contrast to control condition, pre-existing hypokalemia1 with severe COVID-19 reduces the QT interval by 17.39% (0.285 s) and a negative T-peak of 0.16 mV is observed i.e. suggestive of ischemia as seen in **Figure 1(iii)**. HCQ drug does not have any noteworthy effect other than slight reduction of T-peak to  $-0.14$  mV.

In hypokalemia2 in **Figure 1(iv)**, the QT interval is prolonged by 10.14% (0.380 ms) but T-peak reduced by 4.19% (0.217 mV) is observed, and HCQ

exposure increases 18.84% (0.410 ms) QT interval with 12.58% (0.255 mV) increase in T-peak. On considering hypokalemia2 and *mild* COVID-19, the QT interval increases by 2.89% (0.355 s) while T-peak reduces by 37.74% (0.141 mV) in comparison to control, and HCQ inclusion, prolonged QT interval by 10.14% (0.380 s), but reduce the T-peak by 23.17% (0.174 mV). Similar to the hypokalemia1 and COVID-19 scenario, the hypokalemia2 and *severe* COVID-19 we observed, a negative T-peak (0.156 mV) with 13.04% (0.300 s) QT interval reduction. Here too, HCQ has no significant effect, other than a slight increase in the QT interval (0.305 s) and T-peak (0.126 mV).

Finally, in hypokalemia3, **Figure 1(v)**, the QT interval is prolonged by 13.04% (0.390 ms) while the T-peak is reduced by 7.28% (0.210 mV), similar to hypokalemia2 observation. In HCQ presence, the QT interval increases by 23.18% (0.425 ms) and the T-peak increases by 8.61% (0.246 mV) comparing to control. *Mild* COVID-19 has the effect of increasing the QT interval by 5.79% (0.365 s) and reducing the T-peak by 41.28% (0.133 mV). HCQ treatment further prolongs the QT interval by 14.49% (0.395 s) and reduces T-peak by 25.82% (0.168 mV). Similarly for *severe* COVID-19 with hypokalemia3, a negative T-peak of  $-0.155$  mV with 10.14% QT interval reduction (0.310 s) is observed, and on adding HCQ, the QT interval increases to 0.320 s and the T-peak becomes slightly less negative at 0.121 mV. Thus, it can be summarized that irrespective preexisting hypokalemic's severity level, severe COVID-19 can proliferate the risk factor due inverted T-wave presence, that implies the ischemia occurrence.

### 3.1 Arrhythmogenesis effect of HCQ on COVID-19 infected tissue including and excluding hypokalemia

#### 3.1.1 Premature pacing sequence protocol

The scientific community has well accepted that early or late repolarization of the ventricular myocytes manifest due to ionic imbalances and are regulated by different mechanisms; which are involved in or responsible for various life-threatening cardiac diseases. Further, to understand the arrhythmia mechanism, cardiac tissue is paced with premature beats (PBs) in between the normal pacing beats of 800 ms. Three consecutive PBs (single or two PBs are not effective in creating an arrhythmia) are applied to strive in initiating an arrhythmic pattern. PBs duration is determined as the period the endo cell comes out of the refractory state and are re-excitable. The subsequent sections describe the possibility of occurrence of arrhythmia on pacing the tissue with PBs in *mild* and *severe* COVID-19 configurations, comorbid hypokalemia and on inclusion of HCQ.

#### 3.1.2 Arrhythmogenesis response for mild and severe COVID-19 cardiac tissue: when treated with HCQ

**Figure 2** shows the pseudo-ECG on including *mild* and *severe* COVID-19 conditions and on HCQ exposure to cardiac tissue. Under *mild* COVID-19, three PBs of each 295 msec duration are applied after the first beat. The cardiac tissue's mid cells are in a repolarising state when the first PB is applied. This causes the depolarisation from the first PB to travel upward along the endo layer and later depolarise the mid and epi layer, which results in a negative T-wave (**Figure 2(i)**). The depolarisation wavefront from the second PB is not able to excite the cells in the epi layer as they are in a refractory state and this appears as a STE. Further, when the third PB occurs, an inverted T-wave is created as the mid and epi cells depolarize simultaneously. Later in both cases, normal pacing pulses resumed at 1.6 sec and HCQ



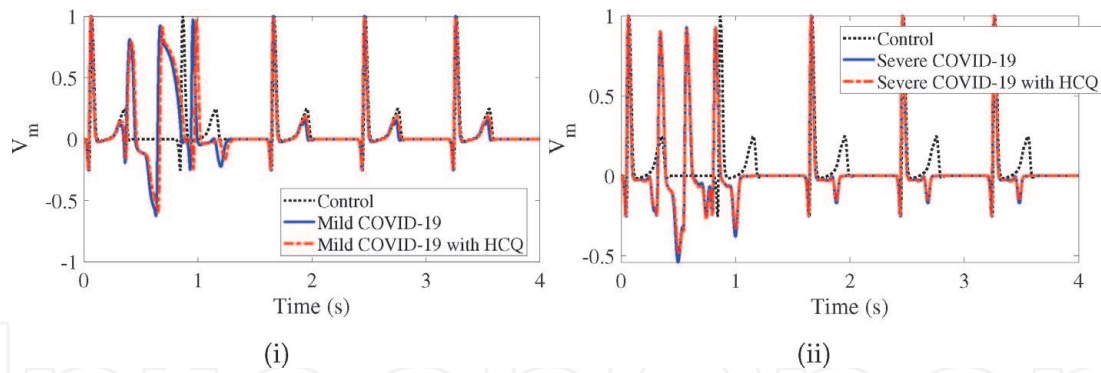


**Figure 2.**

*Pseudo ECG for i)mild COVID-19 and HCQ ii)severe COVID-19 and HCQ.*

presence shows a similar trend. This finding is in line with Wang et al. [14] study, where a  $10 \mu\text{M}$  HCQ dosage prolonged the cells APD but did not induce an arrhythmia on decreasing the pacing interval.

In *severe* COVID-19, the three PBs are applied for every 250 msec, that leads to increase in the negative T-peak amplitude, due to the changes in depolarisation and repolarisation pattern; similar to the first PB in mild COVID-19 case. The first and third PBs increases the amplitude of negative T-peak compared to the second PB. The normal ECGs are resumed at 1.6 sec in both scenarios. Results infers that an inverted T-wave morphology (representative of ischemia) can be used as a bio-marker for *severe* COVID-19 conditions. Further, HCQ drug causes negligible modifications in the voltage propagation patterns and no effect has been observed in the ECG compared with control.

### 3.1.3 Arrhythmogenesis mechanism for the pre-existing Hypokalemia of COVID-19 cardiac tissue: when treated with HCQ

To investigate the impact of COVID-19, pseudo ECGs as shown in **Figure 3** are generated on pacing the tissue with PBs in the presence of different degree of Hypokalemia, severity of COVID-19 and on including HCQ.

**Hypokalemia1 Infected with COVID-19, with and without HCQ:** The tissue is regularly paced every 800 msec. After the first pacing pulse, three premature beats each of 305 msec duration are applied at the same pacing site as indicated in **Figure 3(i)**. It is observed that in the case of hypokalemia1, reentrant activity is generated from 0.37 sec to 1.39 sec and normal beats are resumed from 1.6 sec. On including HCQ and applying three PBs at 325 msec duration each, reentrant activity is generated from 0.38 sec to 2.2 sec and it resumes to normal from 2.4 sec. Hence, there is a 43.96% risk in the arrhythmic activity.

In **Figure 3(ii)**, hypokalemia1 and *mild* COVID-19 conditions are included in the tissue, three PBs each of 295 msec are applied after the first beat. The regular pacing interval is 800 msec. When the tissue is excited due to the first PB, the cells in top of endo layer and those in mid and epi layers are in repolarising state. Thus, the wavefront from first PB travels upwards along the endo layer and propagates into the mid and epi layer. When the second PB occurs at 0.59 sec, the mid and epi cells are in repolarising state, thus the wavefront propagates along the endo layer and then enters into the mid and epi layer from the bottom once they come out of refractory state. A similar excitation pattern is observed after the third PB is applied. These changes in depolarisation and repolarisation appears as an arrhythmic-like activity from 0.355 sec to 1.24 sec in the pseudo ECG and normal beats are resumed from 1.6 s. Therefore, it is to be noted that the reentrant activity is not generated. On including HCQ at 305 msec duration of three premature beats,

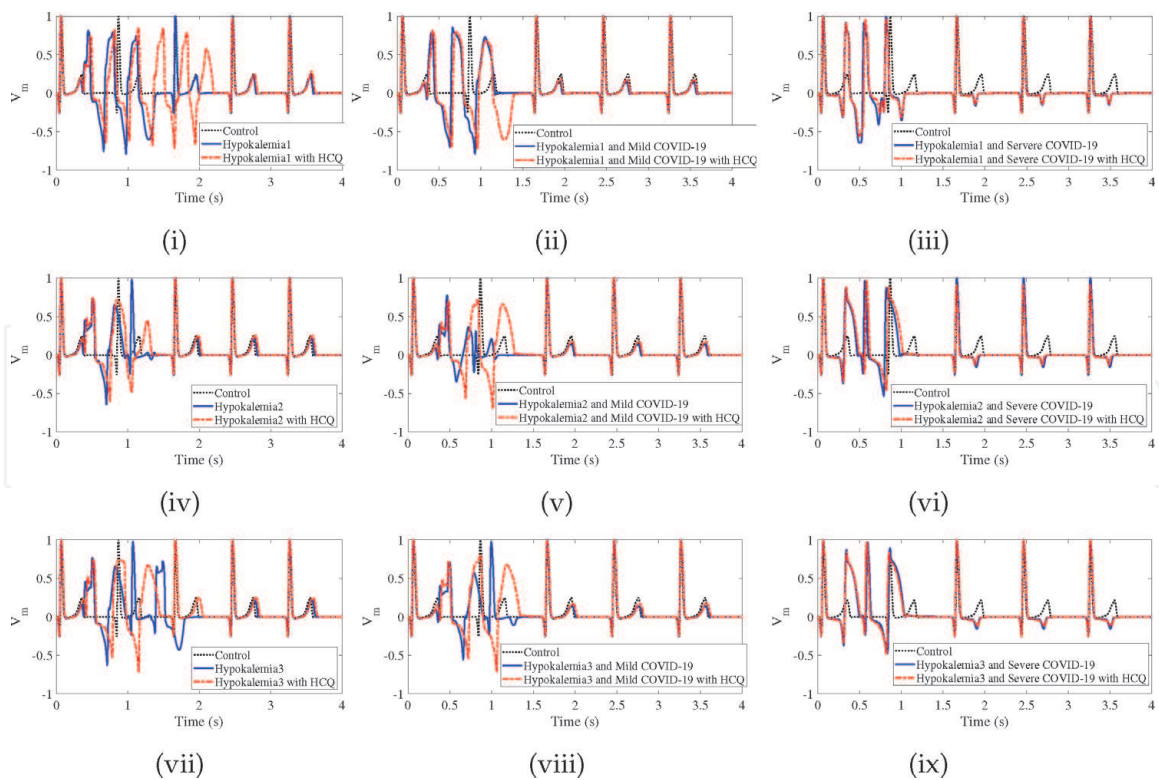


**Figure 3.**  
 Pseudo ECG for i) Hypokalemia<sub>1</sub> and treated with HCQ, ii) Hypokalemia<sub>1</sub> with mild COVID-19 and treated with HCQ iii) Hypokalemia<sub>1</sub> with severe COVID-19 and treated with HCQ iv) Hypokalemia<sub>2</sub> and treated with HCQ v) Hypokalemia<sub>2</sub> with mild COVID-19 and treated with HCQ vi) Hypokalemia<sub>2</sub> with severe COVID-19 and treated with HCQ, vii) Hypokalemia<sub>3</sub> and treated with HCQ, viii) Hypokalemia<sub>3</sub> with mild COVID-19 and treated with HCQ ix) Hypokalemia<sub>3</sub> with severe COVID-19 and treated with HCQ.

a similar type of waveform is generated from 0.365 sec to 1.395 sec and normal beats are resumed from 2.4 sec. On the other hand, hypokalemia<sub>1</sub> infected with *severe* COVID-19, the absence of HCQ creates a reentrant pattern from 0.315 s to 1.045 s on pacing the tissue with 3 PBs each of 250 ms duration as seen in **Figure 3(iii)**. On including HCQ and applying the same pacing protocol, reentry is not generated in the tissue. However, the excitation by the PB creates a similar appearance of ECG waveform. This difference can be seen in **Figure 3(iii)**. This shows that HCQ plays a vital role in pre-existing hypokalemia<sub>1</sub> with COVID-19 cases.

**Hypokalemia<sub>2</sub> Infected with mild COVID-19, with and without HCQ:** Applying three PBs each of 330 msec duration in between the normal pacing pulses in presence of hypokalemia<sub>2</sub> does not generate any re-entrant activity as seen in **Figure 3(iv)**. The third PB at 0.99 sec generates a negative T-peak of 0.056 mV and the normal activity is resumed from 1.6 sec. However, in presence of HCQ with 355 msec PBs, reentrant activity is generated from 0.4 sec to 1.34 sec and the regular pacing sequence is resumed at 1.6 sec.

Hypokalemia<sub>2</sub> and *mild* COVID-19 conditions are included in the tissue and paced with PBs as shown in **Figure 3(v)**. Reentrant activity is observed in the pseudo ECG after pacing with three PBs each of 300 msec duration from 0.355 sec to 0.935 sec. In order to understand the detailed arrhythmogenesis mechanism in hypokalemia<sub>2</sub> with *mild* COVID-19 conditions, voltage maps of cardiac tissue are shown in **Figure 4** starting from the application of the first PB at 0.300 sec. At this time, the endo cells at the top and the M-cells and epi cells are still in repolarizing state. The depolarisation wave created from this first PB is shown in **Figure 4(a)** at 0.31 sec. This wave proceeds upwards along the endo layer by which time the M-cells are returning to rest state as seen in **Figure 4(b)**. The wavefront then travels along the entire length of endo layer and reenters the mid and epi layers as seen in

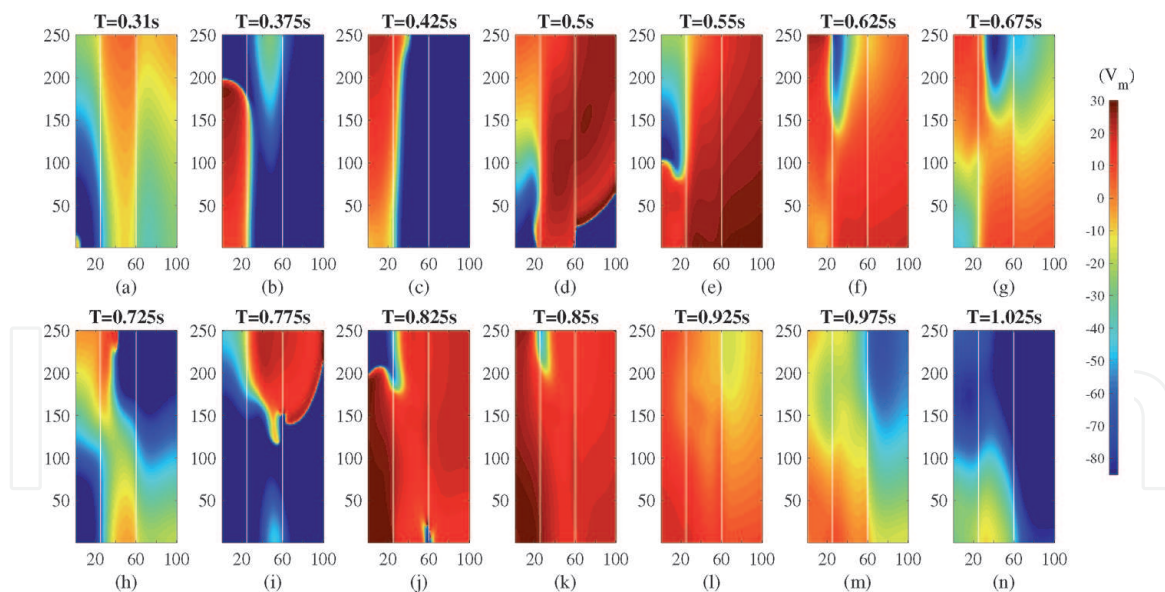


**Figure 4.**  
Voltage maps on applying PBs in Hypokalemia2 with mild COVID-19.

**Figure 4(c)** and **(d)**. This wavefront then reenters into the endo layer at the bottom of the tissue and travels upwards along the endo layer as seen in **Figure 4(e)** and **(f)**. The second PB is applied at 0.6 sec and during this time the endo cells are already depolarised. This wavefront re-enters into the mid and epi layers by which time the mid and epi cells have repolarised as seen in **Figure 4(g)**–**(i)**. The wavefront depolarises cells in mid and epi layers and reenters endo layer as seen in **Figure 4(j)**–**(k)**. The third PB is applied at 0.9 sec and the cells at the pacing site are already depolarised. The cells start repolarising from the epi, mid and endo with cells at the bottom of the endo and mid layer repolarising last as seen in **Figure 4(ii)** **(l)**–**(n)**. All the cells finally repolarise at 1.085 sec.

On adding HCQ and pacing the tissue with 3 PBs, each of 330 msec duration, in between the regular pacing interval of 800 msec, although arrhythmic-like activity is observed from 0.37 sec to 1.295 sec in the pseudo ECG, this is due to the depolarisation and repolarisation sequence of the cells in the tissue and not because of reentry. Normal beats are resumed from 1.6 sec.

In case of *severe* COVID-19 conditions, the application of three PBs each of 250 msec, gives rise to the pseudo ECG shown in **Figure 3(vi)**. The excitation of the first and third PB appear representative of an STE. On introducing HCQ, a similar ECG waveform is observed and no reentry of wavefront is observed.

**Hypokalemia3 Infected with COVID-19, with and without HCQ:** Similarly, in case of hypokalemia3, reentrant activity is not generated when pacing the tissue with 335 msec duration PBs as seen in **Figure 3(vii)**. Inclusion of HCQ causes reentrant activity to appear from 0.415 sec to 1.45 sec on pacing with PBs of 355 msec duration. The regular pacing sequence is resumed at 1.6 sec. Even though HCQ drug is not intended for hypokalemia treatment, here we attempted to understand the role of HCQ in hypokalemia. Result infers that the presence of HCQ is pro-arrhythmic under all severity levels of hypokalemic and would have to be used with caution in such scenarios.

**Figure 3(viii)** shows the pseudo ECG on including Hypokalemia3 and *mild* COVID-19 conditions in the tissue and pacing with PBs. No reentrant activity is observed even after pacing with three PBs each of 310 msec duration. Similarly, on adding HCQ and pacing the tissue with 3 PBs, each of 330 msec duration, in between the regular pacing interval of 800 ms, no reentrant activity is generated. Normal beats are resumed from 1.6 sec. Under hypokalemia3 and *severe* COVID-19



conditions, the application of three PBs each of 265 ms, gives rise to the pseudo ECG shown in **Figure 3(ix)**. Similar to earlier case of hypokalemia2 and severe COVID-19, the excitation of the first and third PB appear representative of an ST-elevation as the epi cells are not depolarised.

#### 4. Dosage effects in COVID-19 infected cardiac tissue: HCQ and with AZM

To understand the influence of different dosages of HCQ alone and in combination with AZM in the COVID-19 infected cardiac tissue, the cardiomyocyte's ionic current parameters are varied based on the clinical study reported by Wang et al., [21], and listed in **Table 3**. To the best of the author's knowledge, prior art studies have not considered the role of temperature (fever) arising due to COVID-19; in this study, we configure the computational model of the ventricular tissue with an elevated temperature of 313.15 Kelvin.

The ECG parameters, namely QT interval, T-peak and QRS duration are extracted from the pseudo ECG and tabulated in **Table 4**. Here, the cardiac tissue is paced with three consecutive premature beats (PBs) with a regular pacing interval of 800 ms (75 bpm). Initialization of the first PB in each case is determined as the endo cell's period comes out of the refractory state and re-excitable. The consecutive beats get reduced by 10 msec. We further extended it in the presence of PBs in *mild* and *severe* COVID-19 to determine the arrhythmia occurrence for various HCQ dosages and with AZM.

In the control ventricular condition, the QT interval is observed to be 0.350 sec, T-peak is 0.232 mV and the QRS duration is 0.07 sec. In the case of adding 1  $\mu$ M, 10  $\mu$ M, and 100  $\mu$ M HCQ, the QT interval increases by 1.42%, 11.43%, and 44.28%, respectively, as shown in **Figure 1(i)**. However, the T-peak decreases by 10.35% and 0.85% under 1  $\mu$ M and 100  $\mu$ M HCQ, but, in 10  $\mu$ M, it increases by 18.10%. Also, QRS duration increased by 7.14% in both 1  $\mu$ M and 10  $\mu$ M HCQ and by 21.4% in 100  $\mu$ M HCQ. Application of PBs in the 1  $\mu$ M HCQ or 10  $\mu$ M HCQ configuration, it gives rise to premature ventricular complexes (PVCs), as seen in **Figure 1(ii)** and the regular pacing sequence resumes at 2.4 sec. The appearance of PVC is due to the change in the repolarisation sequence with endo and mid cells repolarising first, followed by the epi cells. For the 100  $\mu$ M HCQ config, the three PBs gives rise to

Current	HCQ (1 $\mu$ M)	HCQ (10 $\mu$ M)	HCQ (100 $\mu$ M)
$I_{Na}$	22%	35%	55%
$I_{CaL}$	12%	12%	40%
$I_{Kr}$	18%	55%	85%
$I_{K1}$	10%	20%	80%
	HCQ (1 $\mu$ M) and AZM	HCQ (10 $\mu$ M) and AZM	HCQ (100 $\mu$ M) and AZM
$I_{Na}$	18%	22%	38%
$I_{CaL}$	10%	15%	30%
$I_{Kr}$	30%	62%	90%
$I_{Ks}$	18%	20%	22%
$I_{K1}$	10%	30%	82%

**Table 3.**  
 Ionic currents for different dosages of HCQ and with AZM represented by in-vitro study [21].



Dosage ( $\mu\text{M}$ )	Medication	Disease Condition	QT interval (sec)	T peak (mV)	QRS duration (sec)
	No Medication	Control	0.350	0.232	0.070
		<i>Mild</i> COVID	0.325	0.152	0.070
		<i>severe</i> COVID	0.275	-0.170	0.070
1	HCQ	Control	0.355	0.208	0.075
1	HCQ	<i>Mild</i> COVID	0.330	0.110, 0.124	0.075
1	HCQ	<i>severe</i> COVID	0.265	-0.206	0.070
1	HCQ with AZM	Control	0.375	0.24	0.070
1	HCQ with AZM	<i>Mild</i> COVID	0.350	0.151	0.070
1	HCQ with AZM	<i>severe</i> COVID	0.285	-0.194	0.065
10	HCQ	Control	0.390	0.274	0.075
10	HCQ	<i>Mild</i> COVID	0.365	0.194	0.075
10	HCQ	<i>severe</i> COVID	0.290	-0.137	0.070
10	HCQ with AZM	Control	0.420	0.319	0.070
10	HCQ with AZM	<i>Mild</i> COVID	0.390	0.227	0.070
10	HCQ with AZM	<i>severe</i> COVID	0.300	-0.119	0.065
100	HCQ	Control	0.505	0.230	0.085
100	HCQ	<i>Mild</i> COVID	0.450	0.159	0.090
100	HCQ	<i>severe</i> COVID	0.345	-0.075	0.080
100	HCQ with AZM	Control	0.630	0.317	0.075
100	HCQ with AZM	<i>Mild</i> COVID	0.555	0.220	0.075
100	HCQ with AZM	<i>severe</i> COVID	0.355	-0.05	0.070

**Table 4.**

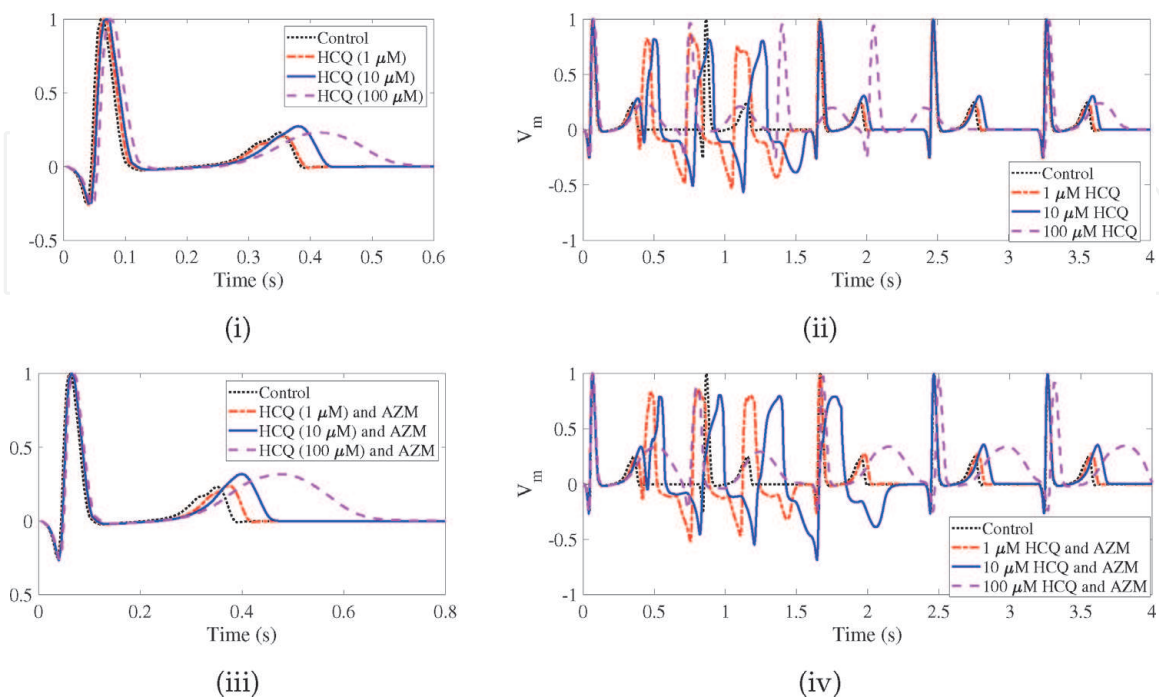
Surrogate biomarker such as QT interval, T-peak and QRS duration of controlled, mild and severely infected COVID ventricle in response to various HCQ doses (1, 10 and 100  $\mu\text{M}$ ) alone or with 1  $\mu\text{M}$  AZM [21].

similar ECG complexes (with positive widened T-waves) as that in usual pacing. The regular beat resumes after a long pause at 3.3 sec.

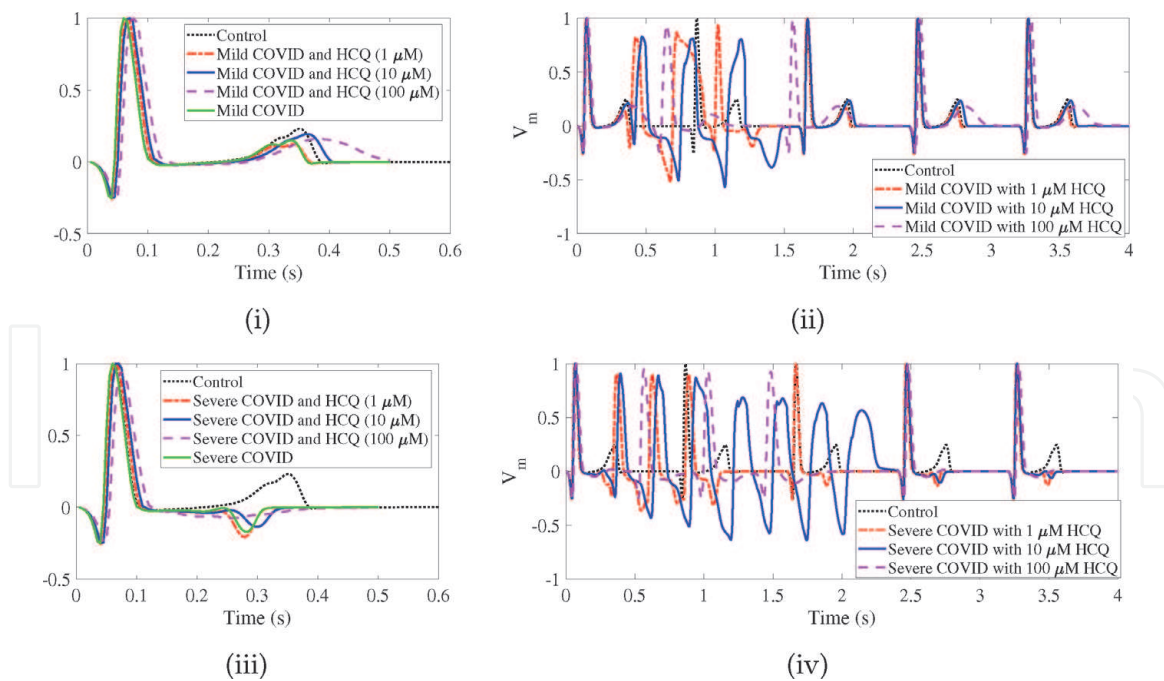
Further, on the inclusion of 1  $\mu\text{M}$  AZM with each of the 1  $\mu\text{M}$ , 10  $\mu\text{M}$  and 100  $\mu\text{M}$  HCQ config, the QT interval prolongs by 7.14%, 20% and 80% respectively, in the control ventricle as shown in **Figure 1(iii)**. Likewise, the T-peak increases by 3.87%, 37.5% and 36.63% under AZM in combination with 1  $\mu\text{M}$ , 10  $\mu\text{M}$  and 100  $\mu\text{M}$  HCQ respectively. However, the QRS duration remains the same in both 1 $\mu\text{M}$  and 10  $\mu\text{M}$  HCQ, but increases by 7.14% in 100  $\mu\text{M}$  HCQ. Additionally, PVCs arise due to the inclusion of PBs in the combination of 1  $\mu\text{M}$  HCQ and AZM, and regular pulses resume at 1.6 sec. The occurrence of PVCs increases in the presence of PBs in 10  $\mu\text{M}$  HCQ, as seen in **Figure 1(iv)**. This effect is due to the change in repolarisation sequence of the cells, specifically occurring from endo to mid and epi. Regular

pulses resume at 2.4 sec. Although no reentry is generated in the tissue, the appearance of PVCs is a precursor to the development of arrhythmia. This finding is in line with the Wang et al., [14], where a dosage of 10  $\mu\text{M}$  HCQ prolonged the APD of cells but did not induce an arrhythmia in tissue on decreasing the pacing interval. Further, the combination of HCQ and AZM created arrhythmic activity. Although no arrhythmic event was generated in the presence of 100  $\mu\text{M}$  HCQ, widened T-waves occurred. Such broad-based and symmetrical T-waves, usually with increased amplitude, are termed as hyperacute T-waves and often associated with a depressed ST are a sign of acute ischemia (**Figure 5**) [22].

In the mild COVID-19 scenario, the QT interval becomes shortened by 7.14% (0.325 sec), and the T-peak decreases by 34.48% while the QRS duration remains unchanged as shown in (**Figure 6(i)**). While using 1  $\mu\text{M}$  HCQ, the model's outcome, Pseudo ECG's QT interval increases by 1.43% with a double notch T-peak of 0.124 mV and 0.110 mV. For the 10  $\mu\text{M}$ , the pseudo-ECG prolongs the QT interval and increases the T-peak by 11.42% and 18.10%, respectively. When HCQ dosage is 100  $\mu\text{M}$ , the QT interval raises by 35.71% with a 3.02% T-peak increase and 21.4% prolongation of QRS duration. However, in the case of 1  $\mu\text{M}$  and 10  $\mu\text{M}$  HCQ, QRS duration increases by 7.14%. In the arrhythmogenesis test, three reduced duration PBs are applied; when the first PB is applied; the mid and epi cells in the tissue start to repolarization due to the excitation from the previous beat, as a consequence, the wave propagates upward along with the endo and mid-layers, and lastly, it enters the epi layer of the cardiac tissue. Succeeding that, the wavefront repolarizes from the endo, mid and epi layer with the cells located at the top of the epi layer repolarizing last, resulting in an inverted T-wave. During the second PB excitation (0.8 sec), the wavefront depolarizes the endo and mid-layer but is not able to excite the epi layer cells as they are in a refractory state and this results in an ST-segment elevation in the ECG, as indicated in (**Figure 6(ii)**). For the last PB, yet another PVC occurs and then regular beats resume at 1.6 sec. In the case of 10  $\mu\text{M}$  HCQ, due to the change in repolarization pattern, PVCs occur, yet they do not lead to the



**Figure 5.** Pseudo ECGs generated (i) in control ventricle treated with HCQ, (ii) on pacing with PBs in presence of HCQ, (iii) in control ventricle treated with HCQ and 1  $\mu\text{M}$  of AZM, (iv) on pacing with PBs in presence of HCQ and 1  $\mu\text{M}$  of AZM.


**Figure 6.**

Pseudo ECGs generated (i) in mild COVID-19 infected ventricle treated with HCQ, (ii) on pacing the mild COVID-19 infected ventricle with PBs with HCQ inhibition, (iii) in severe COVID-19 infected ventricle treated with HCQ, (iv) on pacing the severe COVID-19 infected ventricle tissue with PBs in presence of HCQ.

formation of re-entrant patterns. When PB's are applied in 100  $\mu\text{M}$  HCQ setup, ECG complexes with widened T-waves are observed.

When AZM was supplemented with 1  $\mu\text{M}$  HCQ, 10  $\mu\text{M}$  HCQ and 100  $\mu\text{M}$  HCQ, the QT interval prolongs by a percentage of 7.14, 18.57 and 65.71 respectively, under *mild* COVID conditions (**Figure 6**(iii)). Furthermore, the T-peak increases by about 31% in the combination of AZM and 10  $\mu\text{M}$  HCQ or 100  $\mu\text{M}$  HCQ in comparison to *mild* COVID while there is negligible effect in 1  $\mu\text{M}$  HCQ. Even though the QRS duration remains unchanged for 1  $\mu\text{M}$  and 10  $\mu\text{M}$ , it increases by 7.14% in 100  $\mu\text{M}$  HCQ with 1  $\mu\text{M}$  AZM. On pacing with PBs, PVCs occurred in both 1  $\mu\text{M}$  HCQ and 10  $\mu\text{M}$  HCQ conditions, and the regular pulses resume at 1.6 sec as shown in **Figure 6**(iv). When AZM is supplied with 100  $\mu\text{M}$  HCQ and on applying PBs, no arrhythmic activity appeared in spite of the presence of the hyper-acute T-waves.

In *severe* COVID-19 configuration, the QT interval reduces by 21.48% (0.275 sec) with a negative T-wave peak of  $-0.17$  mV and QT depression as shown in **Figure 6**(v). This negative T-peak episode might be the representation of ischemia, which is in line with the clinical ECG recordings. [23]. On treating with 1  $\mu\text{M}$  HCQ, the QT interval reduces by 2.85% in comparison to severe COVID-19 and the negative T-peak increases by 15.51%. In contrast, under 10  $\mu\text{M}$  HCQ, the QT interval increase by 4.28%, with a 14.22% reduction in T-peak. When the tissues are treated with 100  $\mu\text{M}$  HCQ, the QT interval prolongs by 20%, with an immense reduction in the T-peak (i.e.) 40.98% in comparison to severe COVID-19. Here, the QRS duration is increased by 14.28% in 100  $\mu\text{M}$  HCQ; while remaining unchanged at other dosages. In *severe* COVID-19, the inclusion of 1  $\mu\text{M}$  HCQ and premature pacing sequence creates ECG complexes with increased negative T-peak amplitude due to the changes in the repolarisation pattern as seen in **Figure 2**(vi). The regular pulses are resumed after a long pause at 1.6 sec. In contrast, on including 10  $\mu\text{M}$  HCQ and pacing the tissue with the first PB, the M-cells at the top of the tissue are still in the repolarising state. Therefore, the wave travels upwards along with the endo and mid-layer before entering the epi layer. This creates a change in the repolarisation pattern with endo cells repolarising first, followed by mid and epi cells. A similar



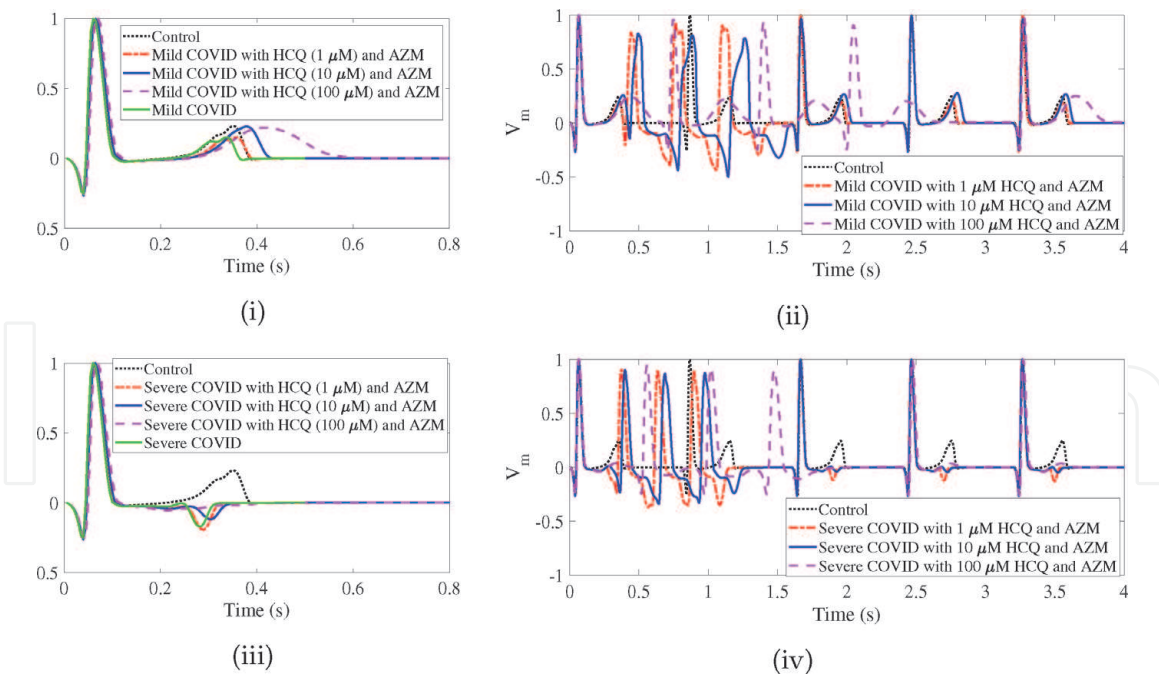


**Figure 7.** Pseudo ECGs generated (i) in mild COVID-19 infected ventricle treated with HCQ and 1  $\mu\text{M}$  AZM, (ii) on pacing the mild COVID-19 infected ventricle with PBs in presence of HCQ and 1  $\mu\text{M}$  AZM, (iii) in severe COVID-19 infected ventricle treated with HCQ and 1  $\mu\text{M}$  AZM, (iv) on pacing the severe COVID-19 infected ventricle tissue with PBs in presence of HCQ and 1  $\mu\text{M}$  AZM.

activation pattern occurs on applying the second PB. When the third PB endures, the epi cells are repolarising; thus, the wavefront travels upwards along with the endo and mid-layer and re-enters the epi layer from the top. Further, the wavefront travels down along the epi layer and re-enters into the mid and endo layer. This reentrant activity creates upward and downward pointing QRS complexes, as shown in 6(vi) and the regular pacing resumes at 2.4 sec following the re-entry termination; for details, refer the voltage maps video1 provided in the Supplementary session. In the case of 100  $\mu\text{M}$  HCQ, no arrhythmic activity or PVCs are observed, although flat T-waves occur, representing the appearance of myocardial ischemia event [24] or hypokalemia [25]. The above result infers that an inverted T-wave morphology (representative of ischemia) can be a biomarker for *severe* COVID-19 screening.

On including AZM, as indicated in **Figure 6(vii)**, the QT interval increases by 2.85%, 7.14% and 22.85% with 1  $\mu\text{M}$  HCQ, 10  $\mu\text{M}$  HCQ and 100  $\mu\text{M}$  HCQ respectively in comparison to *severe* COVID. The T-peak increases by 10.34% in the combination of AZM and 1  $\mu\text{M}$  HCQ while it decreases by 21.98% and 51.72% in 10  $\mu\text{M}$  HCQ and 100  $\mu\text{M}$  HCQ respectively. The QRS duration decreases by 7.14% remains in the combination of AZM and 1  $\mu\text{M}$  or 10  $\mu\text{M}$  HCQ whereas it is unchanged in combination with 100  $\mu\text{M}$  HCQ. On pacing the tissue with PBS, PVCs are observed under 1  $\mu\text{M}$  HCQ and 10  $\mu\text{M}$  HCQ while under 100  $\mu\text{M}$  HCQ, no significant change in the flattened T-waves is observed as seen in as seen in **Figure 6(viii)**. The voltage maps video2 under 100  $\mu\text{M}$  HCQ and AZM is provided in the Supplementary session (**Figure 7**).

## 5. Pacing sequence influence on arrhythmogenesis

In addition, to earlier pacing sequence, after the first beat is introduced, PBs are injected, under two condition, a) three unequal PBs with 800 msec (i.e., HR is 75 beats/min) pulse sequence, b) three equal PBs with 600 msec (i.e., HR is 100 beats/min), tachycardia pulse sequence. In each case, the first PBs duration is determined



based on the refractory state and re-excitability property of bottom endo cells in the tissue. Further, the presence of PBs in mild and severe COVID-19 configurations for various HCQ dosages is applied to examine when an arrhythmia occurs.

Under mild COVID-19 and 1  $\mu\text{M}$  HCQ conditions, three PBs are injected with reduced duration after the first regular beat. The mid and epi cells are still repolarizing when the first PB is applied; this causes the depolarization wave to travel upwards and the endo and mid-layers and later enter the epi layer. Following depolarization, repolarization occurs in the endo, mid and then epi layer, with the cells located at the top of the epi layer repolarizing lastly, leading to a premature ventricular complex (PVC). The depolarization wavefront from the second PB at 0.8-sec proceeds along with the endo and mid layer, however, it cannot excite the epi layer cells as they are in a refractory state, and this appears as an ST-segment elevation. Further, the third PB gives rise to another PVC and at 1.6 sec, the regular beats resume with notched T-waves. For 10  $\mu\text{M}$  HCQ and mild cases, the three PBs give rise to PVCs due to the change in repolarization pattern, and wavefront reentry is absent. However, the QT interval and T-peak increase compared to control. ECG complexes with widened T-waves increased QT interval, and QRS duration is observed on pacing the tissue with three PBs under mild COVID-19 and 100  $\mu\text{M}$  HCQ conditions. In severe COVID-19, the inclusion of 1  $\mu\text{M}$  HCQ or 10  $\mu\text{M}$  HCQ with three PBs for every 245 msec and 265 msec respectively give rise to PVCs with an increased negative/inverted T-peak. This result could be due to the repolarization pattern changes. However, in 100  $\mu\text{M}$  HCQ conditions, no significant change is observed with similar ECG complexes occurring on applying three PBs at a pacing interval of 460 msec. The normal ECGs resumed at 1.2 sec in all three scenarios. Thus, the result inferred that an inverted T-wave morphology (representative of ischemia) could serve as a biomarker for severe COVID-19 conditions.

## 6. Limitation

In this study, we considered a 2D anisotropic transmural ventricular model, in which the entire mid-layer is composed of M-cells with longer APD. However, certain studies have disputed the presence of M-cells [26, 27] and others have debated that they form islands in the endo-mid interface [28, 29]. Here, arrhythmic patterns are generated through a premature pacing sequence. Like other few other studies, [16], here we had not considered using the cross-pacing sequence to simulate an arrhythmia, as the propagation pattern would then travel parallel along the entire length of the ventricle from endo, mid and epi, and it would not mimic the actual depolarisation pattern in the ventricle and thereby result in irregular pseudo-ECG wave. Another option is the generic Short-long-short (SLS) pacing sequences that can initiate TdP pattern [30], which is our future direction. In clinical ECG recordings, self-terminating re-entrant arrhythmia of few cycles may not be considered critical. However, the limited duration of the reentry generated here is due to the consideration of the 2D ventricle model. In a three-dimensional or whole heart model, sustainable ventricular arrhythmias may occur. Finally, we considered 1  $\mu\text{M}$ , 10  $\mu\text{M}$ , and 100  $\mu\text{M}$  of HCQ and 1  $\mu\text{M}$  AZM dosage due to the ionic current percentage variation reported by Wang et al., clinical study.

## 7. Conclusions

This study presents the first complete electrophysiological mechanism of COVID infected ventricle tissue with and without hypokalemia comorbidities and

its responses to HCQ treatment. This model strategically allows more direct studies of ion channel perturbation from clinical observation of infected victims. This study's main conclusion is that when healthy cardiac tissue is infected by COVID, it engenders shorter QT interval, low amplitude or inverted T-waves and ST depression, which could be used as biomarkers. When treated with HCQ, in case of severe COVID-19, there is no significant adverse effect, but in mild COVID-19, QT interval prolongs and T-peak increases in ECG. Secondly, COVID-19 withal to the comorbid cardiac ventricle causes a slight QT interval elongation, notched T-waves in hypokalemia<sup>1</sup>, inverted T-waves in the presence of all severe hypoxia. In particular, the hypokalemic ventricle is prone to arrhythmia in the presence of COVID-19 and the addition of HCQ drug has no significant effects. Increasing the dosage of HCQ has the effect of prolonging the QT interval, and QRS duration and inclusion of AZM magnifies this effect. PVCs could be detected on pacing the tissue with PBs at lower doses of HCQ, and it led to the initiation of reentrant arrhythmia in *severe* COVID-19 conditions. Further, the pacing protocol also determines the appearance of reentry. Thus, the finding of this in-silico model could be considered for HCQ management in patients with pre-existing pathologies.

## Conflict of interest

The authors declare no conflict of interest.

## Nomenclature

$I_{Na}$	Sodium Current
$I_{Kr}$	Rapid delayed rectifier potassium Current
$I_{Ks}$	Slow delayed rectifier potassium Current
$I_{K1}$	Inward rectifier potassium Current
$I_{CaL}$	L-type Calcium Current

## Abbreviations

HCQ	Hydroxychloroquine
ACE2	Angiotensin-Converting Enzyme 2
AZM	Azithromycin
APD	Action Potential Duration
ATP	Adenosine Triphosphate
ECG	Electrocardiogram
PB	Premature Beat
Endo	Endocardial Layer
Mid/M	Midmyocardial Layer
Epi	Epicardial Layer
PVC	Premature Ventricular Complex
SARS-Cov2	Severe Acute Respiratory Syndrome Coronavirus
FDA	Food and Drugs Administration
WHO	World Health Organization
TdP	Torsades de Pointes

IntechOpen

### Author details

Srinivasan Jayaraman<sup>1\*†</sup> and Ponnuraj Kirthi Priya<sup>2†</sup>

1 Life Science Unit, Bio Computational Group, TATA Consultancy Services Limited, Portland, OR, USA

2 Life Science Unit, Bio Computational Group, TATA Consultancy Services Limited, Bangalore, India

\*Address all correspondence to: [srinivasa.j@tcs.com](mailto:srinivasa.j@tcs.com)

† These authors contributed equally.

### IntechOpen

---

© 2021 The Author(s). Licensee IntechOpen. This chapter is distributed under the terms of the Creative Commons Attribution License (<http://creativecommons.org/licenses/by/3.0>), which permits unrestricted use, distribution, and reproduction in any medium, provided the original work is properly cited. 

## References

- [1] Chen CY, Wang FL, Lin CC. Chronic hydroxychloroquine use associated with QT prolongation and refractory ventricular arrhythmia. *Clinical Toxicology*. 2006;44(2):173–175.
- [2] Nord JE, Shah PK, Rinaldi RZ, Weisman MH. Hydroxychloroquine cardiotoxicity in systemic lupus erythematosus: a report of 2 cases and review of the literature. In: *Seminars in arthritis and rheumatism*. vol. 33. Elsevier; 2004. p. 336–351.
- [3] Yao X, Ye F, Zhang M, Cui C, Huang B, Niu P, et al. In vitro antiviral activity and projection of optimized dosing design of hydroxychloroquine for the treatment of severe acute respiratory syndrome coronavirus 2 (SARS-CoV-2). *Clinical Infectious Diseases*. 2020.
- [4] Dan Zhou SMD, Tong Q. COVID-19: a recommendation to examine the effect of hydroxychloroquine in preventing infection and progression. *Journal of Antimicrobial Chemotherapy*. 11 May 2020.
- [5] Capel RA, Herring N, Kalla M, Yavari A, Mirams GR, Douglas G, et al. Hydroxychloroquine reduces heart rate by modulating the hyperpolarization-activated current *I<sub>f</sub>*: Novel electrophysiological insights and therapeutic potential. *Heart rhythm*. 2015;12(10):2186–2194.
- [6] Rodriguez B. Multiscale modeling and simulation investigation of variability and abnormalities in repolarization: Application to drug cardiotoxicity. In: *2010 Computing in Cardiology*. IEEE; 2010. p. 257–260.
- [7] Gautret P, Lagier JC, Parola P, Meddeb L, Mailhe M, Doudier B, et al. Hydroxychloroquine and azithromycin as a treatment of COVID-19: results of an open-label non-randomized clinical trial. *International journal of antimicrobial agents*. 2020;105949.
- [8] Amrita X Sarkar DJC, Sobie EA. Exploiting mathematical models to illuminate electrophysiological variability between individuals. *The Journal of Physiology*;590.
- [9] Mercurio NJ, Yen CF, Shim DJ, Maher TR, McCoy CM, Zimetbaum PJ, et al. Risk of QT Interval Prolongation Associated With Use of Hydroxychloroquine With or Without Concomitant Azithromycin Among Hospitalized Patients Testing Positive for Coronavirus Disease 2019 (COVID-19). *JAMA cardiology*. 2020.
- [10] Li X, Hu C, Su F, Dai J, et al. Hypokalemia and clinical implications in patients with coronavirus disease 2019 (COVID-19). *MedRxiv*. 2020.
- [11] He J, Wu B, Chen Y, Tang J, Liu Q, Zhou S, et al. Characteristic ECG manifestations in patients with COVID-19. *Canadian Journal of Cardiology*. 2020.
- [12] Gattinoni L, Coppola S, Cressoni M, Busana M, Rossi S, Chiumello D. Covid-19 does not lead to a “typical” acute respiratory distress syndrome. *American journal of respiratory and critical care medicine*. 2020;(ja).
- [13] Bennett CE, Anavekar NS, Gulati R, Singh M, Kane GC, Sandoval Y, et al. ST-segment Elevation, Myocardial Injury, and Suspected or Confirmed COVID-19 Patients: Diagnostic and Treatment Uncertainties. In: *Mayo Clinic Proceedings*. Elsevier; 2020. .
- [14] Wang D, Hu B, Hu C, Zhu F, Liu X, Zhang J, et al. Clinical characteristics of 138 hospitalized patients with 2019 novel coronavirus–infected pneumonia in Wuhan, China. *Jama*. 2020;323(11):1061–1069.



- [15] White NJ, Watson JA, Hoglund RM, Chan XHS, Cheah PY, Tarning J. COVID-19 prevention and treatment: a critical analysis of chloroquine and hydroxychloroquine clinical pharmacology. *PLoS medicine*. 2020;17(9):e1003252.
- [16] Ten Tusscher KH, Panfilov AV. Alternans and spiral breakup in a human ventricular tissue model. *American Journal of Physiology-Heart and Circulatory Physiology*. 2006;291(3):H1088–H1100.
- [17] Priya PK, Reddy MR. Study of factors affecting the progression and termination of drug induced torsade de pointes in two dimensional cardiac tissue. *Journal of electrocardiology*. 2017;50(3):332–341.
- [18] Shaw RM, Rudy Y. Electrophysiologic effects of acute myocardial ischemia: a theoretical study of altered cell excitability and action potential duration. *Cardiovascular research*. 1997;35(2):256–272.
- [19] Clayton RH. Re-entry in a model of ischaemic ventricular tissue. In: 2010 Computing in Cardiology. *IEEE*; 2010. p. 181–184.
- [20] Waldo A. Prevalence and Prognostic Significance of Short QT Interval in a Middle-Aged Finnish Population Anttonen O, Junttila MJ, Rissanen H, et al (Pääijä at-Häme Central Hosp, Lahti, Finland; Natl Public Health Inst, Helsinki; Univ of Helsinki; et al) *Circulation* 116: 714-720, 2007. *Year Book of Cardiology*. 2008; 2008:512–513.
- [21] Wang G, Tian X, Lu CJ, Flores H, Maj P, Zhang K, et al. Mechanistic insights into ventricular arrhythmogenesis of hydroxychloroquine and azithromycin for the treatment of COVID-19. *bioRxiv*. 2020.
- [22] Levis JT. ECG diagnosis: isolated posterior wall myocardial infarction. *The Permanente Journal*. 2015;19(4): e143.
- [23] Hanna EB, Glancy DL. ST-segment depression and T-wave inversion: classification, differential diagnosis, and caveats. *Cleveland Clinic journal of medicine*. 2011;78(6):404.
- [24] Morris F, Brady WJ. ABC of clinical electrocardiography: acute myocardial infarction—Part I. *Bmj*. 2002;324(7341): 831–834.
- [25] Chua CE, Choi E, Khoo EY. ECG changes of severe hypokalemia. *QJM: An International Journal of Medicine*. 2018;111(8):581–582.
- [26] Bryant SM, Wan X, Shipsey SJ, Hart G. Regional differences in the delayed rectifier current (I<sub>Kr</sub> and I<sub>Ks</sub>) contribute to the differences in action potential duration in basal left ventricular myocytes in guinea-pig. *Cardiovascular research*. 1998;40(2): 322–331.
- [27] Rodriguez-Sinovas A, Cinca J, Tapias A, Armadans L, Tresanchez M, Soler-Soler J. Lack of evidence of M-cells in porcine left ventricular myocardium. *Cardiovascular research*. 1997;33(2):307–313.
- [28] Antzelevitch C. M cells in the human heart. *Circulation research*. 2010;106(5):815–817.
- [29] Glukhov AV, Fedorov VV, Lou Q, Ravikumar VK, Kalish PW, Schuessler RB, et al. Transmural Dispersion of Repolarization in Failing and Non Failing Human Ventricle. *Circulation research*. 2010;106(5):981.
- [30] Sweeney MO, Ruetz LL, Belk P, Mullen TJ, Johnson JW, Sheldon T. Bradycardia pacing-induced short-long-short sequences at the onset of ventricular tachyarrhythmias: a possible mechanism of proarrhythmia? *Journal of the American College of Cardiology*. 2007;50(7):614–622.